

# Magnetism of a four-center transition-metal cluster revisited

W. Hübner,<sup>1</sup> Y. Pavlyukh,<sup>1,2</sup> G. Lefkidis,<sup>1,\*</sup> and J. Berakdar<sup>2</sup>

<sup>1</sup>*Department of Physics and Research Center OPTIMAS, University of Kaiserslautern, P.O. Box 3049, 67653 Kaiserslautern, Germany*

<sup>2</sup>*Institut für Physik, Martin-Luther-Universität Halle-Wittenberg, 06120 Halle, Germany*

(Received 5 May 2017; revised manuscript received 4 October 2017; published 27 November 2017)

We propose a surprisingly efficient procedure to map a sophisticated treatment of electronic correlations to a few-parameter model Hamiltonian. By pushing first-principles coupled-cluster methods to the limit we get a lucid picture of the electronic excitations responsible for the magnetic interactions in a paradigm  $\text{Ni}_4$  cluster. Using an extended Hubbard model, we demonstrate that the magnetism in this system cannot be explained solely on the basis of spin models but additionally requires consideration of the indirect mechanism involving hopping and on-site repulsion. We present a protocol to extract the corresponding parameters from experiment or calculations.

DOI: [10.1103/PhysRevB.96.184432](https://doi.org/10.1103/PhysRevB.96.184432)

## I. INTRODUCTION

Spin models are a fundamental paradigm of condensed-matter physics, yielding a rich family of magnetically ordered phases [1,2] and playing an important role in the description of high-temperature superconductivity and phases with topological order [3,4]. However, it is rather the exception than the rule that, physically, they are realized as actual spins on a periodic lattice. On the contrary, magnetic interactions can have a number of underlying mechanisms and be realized in physically very different systems such as atoms in optical lattices [1,5,6].

A more microscopic description in which each transition-metal atom is associated with an effective spin can potentially be very accurate in reflecting relevant physical properties; however, the extraction of appropriate magnetic interaction parameters [7] is neither experimentally [8,9] nor theoretically [10–12] trivial.

The problem of determining the exchange coupling constants is mathematically ill posed as there is no unique solution and very often a number of very different models can be attributed to a given system depending on the energy scale of interest. Ruiz *et al.* [10,13,14] circumvent this ambiguity by considering  $n + 1$  single-determinant energies corresponding to different spin distributions in order to determine  $n$  different exchange constants (an overcomplete system). This method can be traced back to the discussion of the broken-symmetry states [15–18]. Once the exchange and other interactions are determined, the spectrum of magnetic excitations can be numerically computed [19–21] or solved analytically [22–25] in simpler cases, or the model can be reduced to a giant spin model [26–28].

Also periodicity is not required [29], and the most interesting magnetic states are those with broken translational symmetry [4] or forming an incommensurate lattice [30]. In this work we focus on the realization of spin models in finite systems [7]. Since the first observations of the quantum tunneling of magnetization [31,32] were faithfully rationalized in terms of a giant spin model [33–36], the term single-molecule magnet became common [37,38]. These experiments stimulated a number of interesting theoretical observations

[39] and, with a continuously growing list of nanomagnets available for investigations [40], lead to the realization that giant spin models are inadequate when different spin multiplets are nested within the ground one [41].

Despite the great progress in the determination of spin Hamiltonians from *ab initio* calculations achieved in recent years [42–44], accurately determining the electronic energy levels, computing their magnetic properties, and, finally, interpreting the results in terms of exchange constants are still difficult whenever more than two magnetic centers are present [15]. The reason is the exponentially growing number of relevant magnetic configurations [45–49].

There exists an enormous body of literature with respect to magnetic order in the Hubbard and related model Hamiltonians, particularly in the development of dynamical mean-field theory [50–52]. However, there is still a lack of knowledge about how to relate high-level quantum-chemical-based calculations for small localized transition-metal systems to sufficiently well suited minimal model Hamiltonians. Therefore, in this work we propose a protocol to map results of *ab initio* calculations onto spin models.

By starting from an extended Hubbard model with the fewest necessary parameters to adequately describe the system [three Hubbard  $U$ , three exchange parameters  $J_i$ , and two hopping parameters  $t_i$ ; see Fig. 4(b) below] and focusing on the low-energy sector we show that the  $J$  are symmetry dependent and strongly renormalized by the on-site Hubbard repulsion. We also establish the importance of the screening effects influencing the magnitude of the Hubbard  $U$  even in small systems, an issue that is often speculated about in the literature but, to the best of our knowledge, has never been demonstrated explicitly. Moreover, we convey the message that our protocol can be used to perform calculations in more general geometries and in the presence of ligands. To this end, we focus on the scenario where competing energy scales are set by the crystal-field splitting and exchange interactions between transition-metal atoms.

This paper is organized as follows. In Sec. II we introduce the model and the full quantum-chemistry results. In Sec. III we introduce the model spin Hamiltonian and the way to downfold it to an analytically manageable size, while in Sec. IV we use our procedure on our *ab initio* results. Finally, we summarize our conclusions in Sec. V.

\*lefkidis@physik.uni-kl.de

## II. SYSTEM AND *AB INITIO* CALCULATIONS

As a paradigm system we choose  $\text{Ni}_4$ . This cluster may exist in different conformations (chain [53], planar [54], or tetrahedral structure [55]). Although in the gas phase the energetically most favorable geometry is probably the tetrahedral structure, the planar one is of utmost interest for applications, where  $\text{Ni}_4$  is brought on surfaces [56]. In this study we assume a planar square geometry with a side length of 2.28 Å, where the onset of electronic band contributions can be observed. While it can be synthesized as a part of larger magnetic molecules involving ligands [57,58] or be deposited on a surface [59], which in both cases leads to a planar geometry, here we consider the bare magnetic cluster. Our system lies in between two extremes: the gas-phase atomic Ni, which can be, up to a point, described with a simple Hubbard Hamiltonian, and the extended ferromagnetic bulk and surface Ni, which can be described with a one-particle, band-structure model.

It is well known that in both solids and molecular systems indirect mechanisms are important. The Goodenough-Kanamori rules, which were originally derived for bulk systems [60–63], allow us to predict the sign of exchange constants based on the population (filled vs half filled) of the  $d$  orbitals and their overlap with the ligand  $p$  states. Although the magnetic interactions mediated by the ligand atoms are neglected, the competing excitations on the  $d$  shells are still fully taken into account. An unexpected finding of the present work is that indirect mechanisms are also present in pure transition-metal systems, as will be demonstrated below based on the form of an effective exchange interaction.

In  $\text{Ni}_4$  the strong static correlations cannot be neglected, and at the same time the molecular symmetry must be taken into account. Considering the competing virtual excitations on the  $d$  shells is a formidable task since correlated calculations with 24 valence orbitals (one  $s$  and five  $d$  for every Ni atom) are at the very limit of current computational capabilities. In fact, we cannot even rely upon the broken-symmetry approach because of the large number of open electronic shells. Thus, the calculation requires careful analysis of dominant electronic configurations.

Our calculations are performed with a Sapporo full-electron basis set of double-zeta quality in  $(16s13p9d2f)/(6s4p3d1f)$  contraction [64]. They yield a Hartree-Fock energy of  $-6026.7698266$  hartrees, whereas the subsequent coupled-cluster (CCSD) calculations with 18 frozen-core electrons on each Ni atom lower this value by  $-1.6604878$  hartrees. Both the Hartree-Fock and the post-self-consistent-field calculations are well converged ( $10^{-7}$ ) using the GAMESS [65] and verified by the ORCA [66] quantum-chemistry packages. Both packages yield identical energy values. The ground state consists of doubly occupied  $d_{xy}$ ,  $d_{xz}$ ,  $d_{yz}$ , and/or  $d_{z^2}$  molecular orbitals, localized on each of the Ni atoms. The  $d_{x^2-y^2}$  molecular orbitals remain unoccupied. Furthermore, there are four bonding occupied states of hybridized  $s$ - $p$  character both below and above the gap.

With preliminary unrestricted-Hartree-Fock (UHF) calculations on a slightly distorted square planar geometry ( $D_{2h}$ ) we identify the ground state as a quintet. This is consistent with the competing  $s^2d^8$  and  $s^1d^9$  valence configurations

of the Ni atoms (also evident in the natural-bond-orbital analysis). However, due to spin contamination of UHF results, it is impractical to use this state as a starting point for correlated calculations. Instead, we start from the closed-shell singlet reference state and calculate 57 many-body states (24 singlets and 33 triplets; see Fig. 1) with the state-of-the-art equation-of-motion coupled-cluster method with single and double excitations [68]. Since all excited many-body states are mainly formed through single excitations from the reference state (additionally corrected by double, triple, and quadruple excitations), one would naively expect that all the singlet-triplet splittings result from magnetic exchange interaction with some constant  $J$ . This conclusion would support the use of the giant spin model and yield an identical splitting proportional to  $J$  in all symmetry classes. However, as a quick glance at Fig. 1(d) reveals, this is generally not the case: The splittings vary too much to be unified with a single  $J$ .

Our *first finding* is that we can clearly divide 34 of our states into three categories by individually inspecting their dominant virtual excitations with respect to their  $d \rightarrow d$  character: (a)  $d_{xz}/d_{yz} \rightarrow d_{x^2-y^2}$ , (b)  $d_{z^2} \rightarrow d_{x^2-y^2}$ , and (c)  $d_{xy} \rightarrow d_{x^2-y^2}$  (Fig. 1); the other states are too mixed. As it turns out, it is possible to match our first-principles results with model Hamiltonians if we use different parameter sets for each of the three categories.

Figure 2 depicts two correlated many-body states. The one in Fig. 2(a) (the energetically lowest  $B_{2g}$  triplet and singlet states) belongs to the absolutely nonproblematic ones. We can easily identify *all*  $d \rightarrow d$  virtual transitions (also compare with the orbitals as expected from group-theory analysis; Fig. 3). Furthermore, both the singlet and the triplet states have very similar compositions (compare the numbers above and below the arrows in Fig. 2), and thus, we can treat them approximately as a singlet-triplet pair with the same spatial part of the orbital function. Figure 2(b) depicts a many-body state which cannot be treated with our model Hamiltonian. The reason is that molecular orbital 61 clearly has a  $p$  and not a  $d$  character (it does not correspond to any of the cases in Fig. 3) and results from hybridization as well as correlations. Hence, we do not consider it in the procedure of extracting the exchange couplings  $J$ .

## III. MODEL HAMILTONIAN

The scope of a spin Hamiltonian is to derive a relatively uncomplicated (if possible, even analytically solvable) system which has most of the characteristics of the real system to be studied. The ingredients of a model can be experimentally measured for an ensemble of molecules, e.g., by fitting  $T\chi(T)$  curves (where  $T$  is the temperature and  $\chi(T)$  is the magnetic susceptibility). They can also be accessed for individual clusters, e.g., with micro- and nanoscale superconducting quantum interference devices (SQUIDS) [69,70].

One major complication with spin Hamiltonians is that they do not take into account the spatial part of the electronic wave function. Thus, although they may very successfully describe some systems, they can fail if the spatial part leads to bond building (even more so when correlations cannot be neglected), which in turn, significantly changes the degeneracy of the electronic states. In the case of  $\text{Ni}_4$  we are dealing

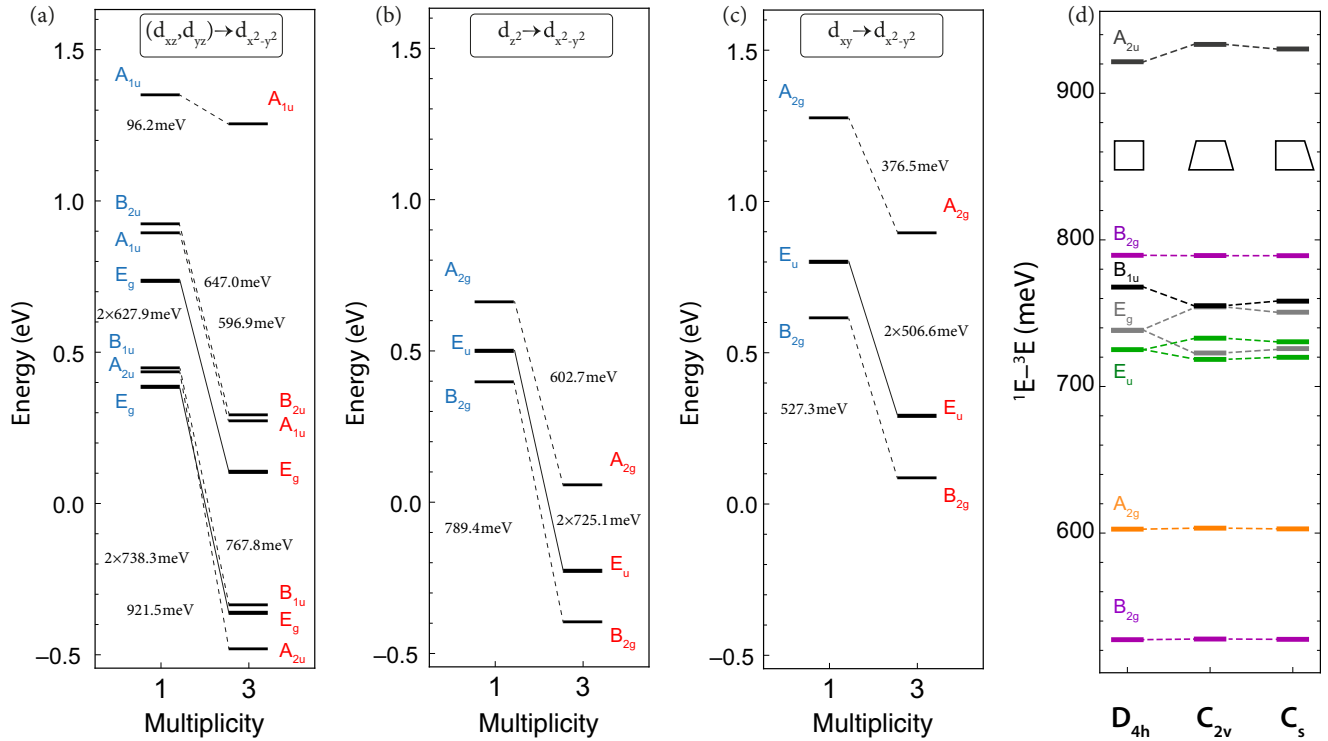


FIG. 1. Many-body-state energies of the first-principles EOM-CCSD calculations in the Ni<sub>4</sub> cluster. Pairs of singlet (in blue) and triplet (in red) states built from the same dominant virtual one-electron excitations (shown in the insets): (a)  $(d_{xz}, d_{yz}) \rightarrow d_{x^2-y^2}$ , (b)  $d_{z^2} \rightarrow d_{x^2-y^2}$ , and (c)  $d_{xy} \rightarrow d_{x^2-y^2}$ . Note that optical selection rules are not relevant to virtual molecular excitations. (d) Summary of the singlet-triplet splittings for the different singlet-triplet pairs as the symmetry of the cluster is gradually lowered ( $D_{4h} \rightarrow C_{2v} \rightarrow C_s$ ). The colors refer to the irreducible representations (see Fig. 4). Note that the doubly degenerate states  $E_g$  and  $E_u$  get split when leaving the perfect square geometry ( $D_{4h}$ ) [67].

with many-body states consisting of  $d$ -character unpaired electrons, which, due to the local crystal field, get split into five categories.

Even without a quantum-chemical calculation one can identify them by applying group theory on the basis of the 20

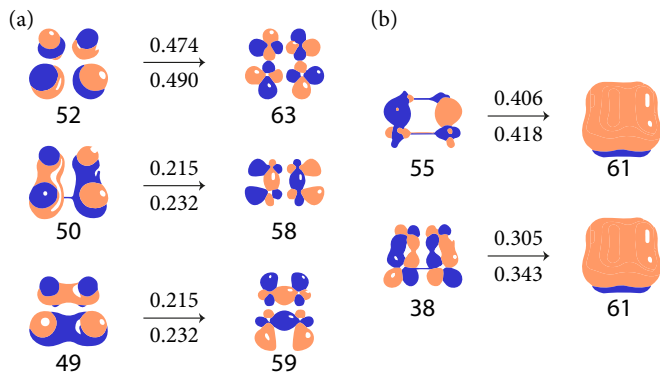


FIG. 2. Main virtual excitations building up the correlated many-body states. The numbers below the Hartree-Fock molecular orbitals indicate their ascending energetic ordering. The numbers above the arrows are the excitation coefficients of the triplets, and those below the arrow are the excitation coefficients of the pertinent singlet states. (a) The energetically lowest  $B_{2g}$  states [see also Fig. 1(b)]. (b) An excited state in which the virtual excitations have a  $d \rightarrow p$  character and which is therefore excluded from our considerations for the spin Hamiltonian.

$d$  orbitals in the  $D_{4h}$  point group. The resulting irreducible representations are shown in Fig. 3. Although one cannot tell beforehand which combinations will have which energies, the actual calculations show that the combinations stemming from the  $d_{x^2-y^2}$  atomic orbitals have the highest energy and are thus the virtual orbitals, while the rest are occupied orbitals. Ultimately, one can build four categories of correlated many-body functions (by excitations starting from one of the occupied orbitals to one empty  $d_{x^2-y^2}$ -character orbital). The irreducible representation of the resulting many-body wave function is the outer product of the irreducible representations of all the occupied orbitals.

From our *ab initio* results we can identify 17 pairs of singlet and triplet states with approximately the same spatial configuration [Figs. 1(a)–1(c)] and thus use them to extract phenomenological parameters for our spin Hamiltonian:

$$\hat{H} = \hat{H}_h + \hat{H}_U + \hat{H}_J. \quad (1)$$

The three terms denote the hopping, the on-site Coulomb, and the exchange interactions, respectively:

$$\begin{aligned} \hat{H}_h &= - \sum_{a,i,j,\sigma} t_{i,j,a} \hat{c}_{i,a,\sigma}^\dagger \hat{c}_{j,a,\sigma} + \text{H.c.}, \\ \hat{H}_U &= \frac{U}{2} \sum_{i,\sigma_1,\sigma_2} \hat{n}_{i,a,\sigma_1} \hat{n}_{i,b,\sigma_2}, \\ \hat{H}_J &= \sum_{i,j,\sigma_1,\sigma_2} J_{i,j,a,b} \hat{c}_{i,a,\sigma_1}^\dagger \hat{c}_{i,b,\sigma_1} \hat{c}_{i,b,\sigma_2}^\dagger \hat{c}_{i,a,\sigma_2}, \end{aligned} \quad (2)$$

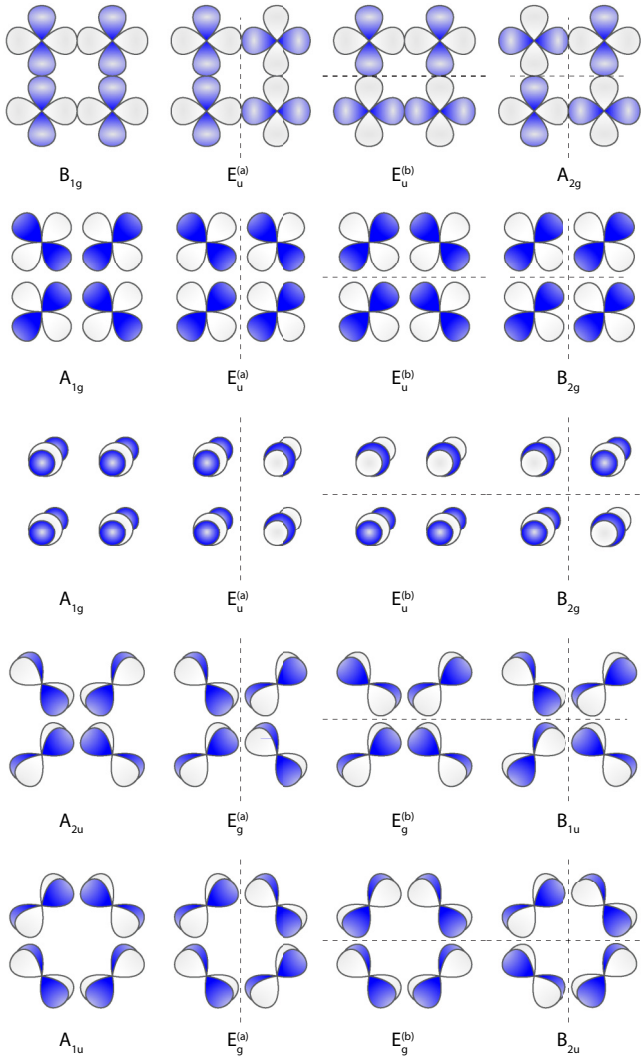


FIG. 3. Top view of the 20  $d$ -character molecular orbitals, combined to form irreducible representations of the  $D_{4h}$  point group. The top row (stemming from  $d_{x^2-y^2}$ ) shows virtual orbitals. The dashed lines represent nodal planes, the number of which is connected to the total energy of the molecular orbital within a group. The depicted orbitals are predicted through group theory and, as such, take into account neither  $p$  or  $s$  hybridization nor correlations.

where  $i$  and  $j$  indicate the sites,  $a$  and  $b$  indicate the orbitals, and  $\sigma_i$  is the spin;  $\hat{n}_{i,a,\sigma_i}$ ,  $\hat{c}_{i,a,\sigma_i}^\dagger$ , and  $\hat{c}_{i,a,\sigma_i}$  are the population, creation, and annihilation operators, respectively. Since our first-principles calculations involve  $d_a \rightarrow d_b$  virtual excitations, we build our model with two spatial orbitals per site (e.g.,  $d_{xy}$  and  $d_{x^2-y^2}$ ), giving rise to 16 spin orbitals in total. In  $\hat{H}_h$  we take into account only nearest-neighbor interactions between the same spatial orbitals; in  $\hat{H}_U$  we account for only on-site interactions with one common Hubbard  $U$ , while in  $\hat{H}_J$  we consider the on-site ( $J_1$ ), the nearest-neighbor ( $J_2$ ), and the next-nearest-neighbor (diagonal,  $J_3$ ) contributions between  $d_a$  and  $d_b$  [Fig. 4(b)].

As an illustrative example we examine the  $d_{xy} \rightarrow d_{x^2-y^2}$  case [Fig. 1(c)]. We start from a basic many-body function  $|\psi_0\rangle$ , in which all eight  $d_{xy}$  orbitals are filled (both spin

up and spin down on all four atoms). The basis of our spin-Hamiltonian is then constructed out of single excitations from  $|\psi_0\rangle$ :

$$|\psi_{i,\sigma}^j\rangle = \hat{c}_{j,d_{x^2-y^2},\sigma}^\dagger \hat{c}_{i,d_{xy},\sigma} |\psi_0\rangle, \quad (3)$$

giving rise to  $2 \times 4 \times 4 = 32$  functions. Here  $i$  and  $j$  denote the site, and  $\sigma$  is the spin. We can block diagonalize the Hamiltonian (1) if we move to a symmetry-adapted basis in which the basis functions belong to the irreducible representations of the system's point group ( $D_{4h}$ ). The total Hilbert space is  $2 \otimes (A_{1g} \oplus 3A_{2g} \oplus B_{1g} \oplus 3B_{2g} \oplus 4E_u)$ . The (unnormalized) spatial parts of the basis functions are

$$\begin{aligned} \phi^{A_{1g}/B_{1g}} &= \psi_1^2 \pm \psi_2^2 \mp \psi_3^2 - \psi_3^2 + \psi_4^4 \pm \psi_3^3 \mp \psi_4^1 - \psi_4^4, \\ \phi_1^{A_{2g}/B_{2g}} &= \psi_1^1 \mp \psi_2^2 + \psi_3^3 \mp \psi_4^4, \\ \phi_2^{A_{2g}/B_{2g}} &= \psi_1^2 \mp \psi_2^2 \mp \psi_3^2 + \psi_3^2 + \psi_4^4 \mp \psi_3^3 \mp \psi_4^1 + \psi_4^4, \\ \phi_3^{A_{2g}/B_{2g}} &= \psi_1^3 + \psi_3^3 \mp \psi_2^4 \mp \psi_4^2, \\ \phi_1^{E_u^+/E_u^-} &= \psi_1^1 \pm \psi_2^2 - \psi_3^3 \mp \psi_4^4, \\ \phi_2^{E_u^+/E_u^-} &= \psi_1^2 \pm \psi_2^2 - \psi_3^4 \mp \psi_3^3, \\ \phi_3^{E_u^+/E_u^-} &= \psi_2^3 \mp \psi_3^2 - \psi_4^1 \pm \psi_4^4, \\ \phi_4^{E_u^+/E_u^-} &= \psi_1^3 - \psi_3^1 \pm \psi_2^4 \mp \psi_4^2. \end{aligned} \quad (4)$$

Both the  $A_{1g}$  and  $B_{1g}$  blocks are two-dimensional (including spin), with energy eigenvalues  $\frac{1}{2}J_2$  and  $-\frac{1}{2}J_2$  for the singlet and the triplet, respectively. Due to strong correlations, however, the lowest singlet-triplet pairs with these irreducible representations that our *ab initio* calculations yield do not have the same spatial wave functions [therefore, they are absent in Fig. 1(c)]. The  $A_{2g}$  and  $B_{2g}$  blocks are six-dimensional, while the  $E_u^+$  and  $E_u^-$  blocks are eight-dimensional. The  $A_{2g}$  and  $B_{2g}$  blocks can be further split into two three-dimensional blocks by separating singlet and triplet states (since the total-spin operator  $\hat{S}^2$  commutes with  $\hat{H}$ ), yielding

$$\hat{H}_{S^2}^{A_{2g}/B_{2g}} = \begin{pmatrix} \frac{1}{2}(gJ_1 - U) & \sqrt{2}t_{\pm} & 0 \\ \sqrt{2}t_{\pm} & \frac{1}{2}gJ_2 & \sqrt{2}t_{\pm} \\ 0 & \sqrt{2}t_{\pm} & \frac{1}{2}gJ_3 \end{pmatrix}, \quad (5)$$

where  $g = \pm 1$  for singlets ( $S^2 = 0$ ) and triplets ( $S^2 = 2$ ), respectively. Here  $t_{\pm} = t_a \pm t_b$  for the  $A_{2g}$  and  $B_{2g}$  blocks, respectively. Out of the three eigenstates of  $\hat{H}_{S^2}^{A_{2g}/B_{2g}}$ , one is an ionic charge-transfer state (also evident from its  $U$  dependence). Ionic states lie energetically very high (several eV) if they originate from  $d \rightarrow d$  excitations and are therefore not present in our first-principles calculations. They can be projected out with the downfolding technique of the Feshbach-Schur map [71]:

$$\hat{H} \rightarrow \hat{H}^{\text{eff}} = \hat{P} \hat{H} \hat{P} + \hat{P} \hat{H} \hat{Q} \frac{1}{\mathcal{E} - \hat{Q} \hat{H} \hat{Q}} \hat{Q} \hat{H} \hat{P}. \quad (6)$$

$\hat{P} = \hat{P}^2$  is the projection operator onto the relevant (desired) subspace, and  $\hat{Q} = \hat{Q}^2 = 1 - \hat{P}$  is the projection operator onto the complementary subspace (to be eliminated).  $\mathcal{E}$  is the energy of the eliminated state. Applying this formalism

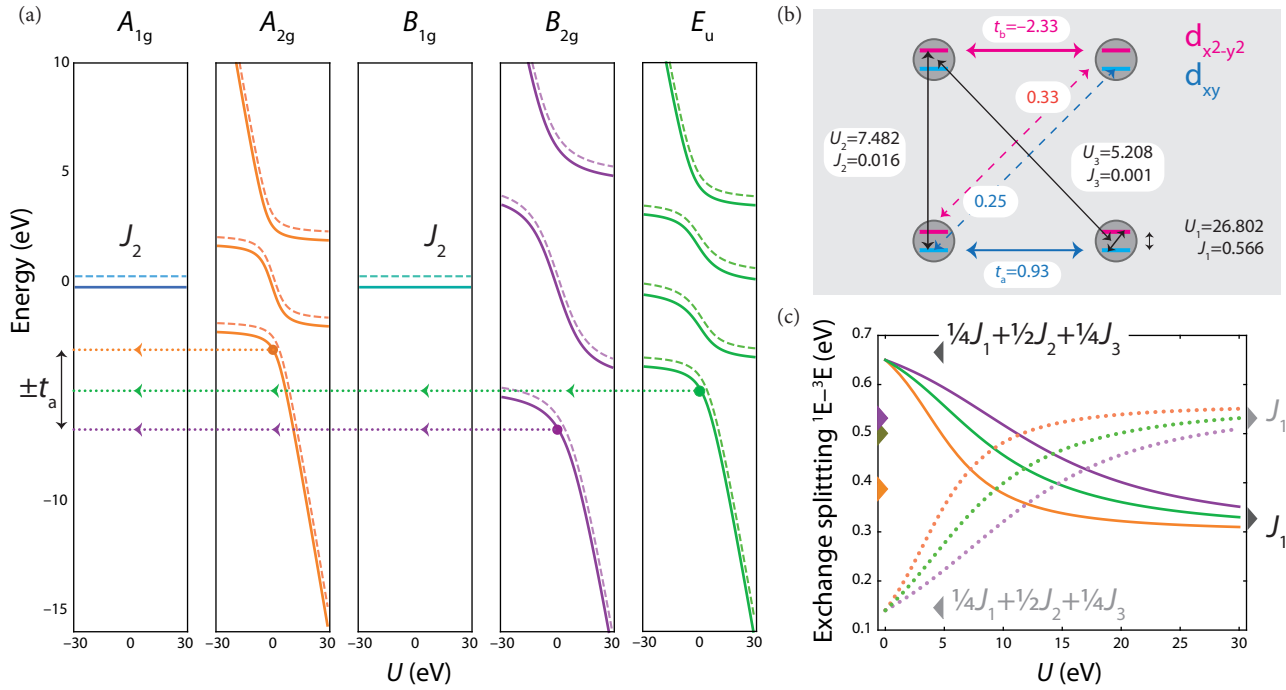


FIG. 4. (a) Energies of singlet (dashed lines) and triplet (solid lines) states of the extended Hubbard Hamiltonian as functions of the Coulomb repulsion parameter for the five irreducible representations created by the virtual excitations  $d_{xy} \rightarrow d_{x^2-y^2}$  [see Fig. 1(c)]. The indicated  $\pm t_a$  values refer to the actual *ab initio* calculations. (b) Schematic of the definitions of the hopping and interaction parameters for the same excitations. The values are *not* extracted from the EOM-CCSD calculations but are directly the bare, noncorrelated integrals between the  $d$  orbitals. (c) Singlet-triplet splittings for two sets of exchange parameters:  $J_1 = 0.3$  eV,  $J_2 = 0.8$  eV,  $J_3 = 0.4$  eV (solid lines) and  $J_1 = 0.56$  eV,  $J_2 = J_3 = 0$  eV (dotted lines).  $t_b = -2.3$  eV and  $t_a = 0.93$  eV for both sets. The colors refer to the different irreducible representations (purple for  $B_{2g}$ , green for  $E_u$ , and orange for  $A_{2g}$ ) and are the same as in (a). The values indicated with the colored triangles refer to the actual *ab initio* calculations [see Figs. 1(a)–1(c)]. The best matching is obtained for  $U = 10$  eV, while  $U = 0$  yields the value  $\frac{1}{4}J_1 + \frac{1}{2}J_2 + \frac{1}{4}J_3$ .

to the Hamiltonian (5), we eliminate the first row and the first column (the element  $H_{11}$  contains the dependence on the Coulomb repulsion  $U$ ). The new effective Hamiltonian is

$$\hat{H}_{\pm}^{\text{eff}} = \begin{pmatrix} \frac{1}{2}gJ_{2,\pm}^{\text{eff}} & \sqrt{2}t_{\pm} \\ \sqrt{2}t_{\pm} & \frac{1}{2}gJ_3 \end{pmatrix}, \quad (7)$$

with  $J_{2,\pm}^{\text{eff}} = J_2 + \frac{8t_{\pm}^2}{g(2\mathcal{E}_i^{(0)} - gJ_1 + U)}$ . As a check, for vanishing exchange ( $J_1 = J_2 = J_3 = 0$ ), the lowest eigenvalues of  $\hat{H}_{S_2}^{\text{eff}}$  indeed reduce to those of  $\hat{H}_{\pm}^{\text{eff}}$ , with no singlet-triplet splitting even in the presence of  $U$ . Thus, the on-site exchange  $J_1$  is important only for small values of the Coulomb repulsion  $U$ , whereas for typically large  $U$  (i.e.,  $U \gg 2t_i$  and  $U \gg J_1$ ),  $J_{2,\pm}^{\text{eff}}$  gets a contribution proportional to  $\frac{8t_{\pm}^2}{U}$ , a form representative of the double-exchange mechanism.

Similarly, in the four-dimensional  $E_u^{\pm}$  sectors we obtain

$$\hat{H}_i^{\text{eff}} = \begin{pmatrix} \frac{1}{2}gJ_{1,i}^{\text{eff}} & t_i^{\text{eff}} & t_+ \\ t_i^{\text{eff}} & \frac{1}{2}gJ_{2,i}^{\text{eff}} & t_- \\ t_+ & t_- & \frac{1}{2}gJ_3 \end{pmatrix}, \quad (8)$$

where  $J_{1,i}^{\text{eff}} = J_2 + \frac{4t_{\pm}^2}{g(2\mathcal{E}_i^{(0)} - gJ_1 + U)}$ ,  $J_{2,i}^{\text{eff}} = J_2 + \frac{4t_{\pm}^2}{g(2\mathcal{E}_i^{(0)} - gJ_1 + U)}$ , and  $t_i^{\text{eff}} = \frac{1}{2}g(J_{1,i}^{\text{eff}} - J_{2,i}^{\text{eff}}) \frac{t_+ t_-}{t_+^2 - t_-^2}$  for  $i = 1$  or  $2$ .

Equations (7) and (8) exemplify our *second finding*: In every symmetry subspace, one can construct similar model Hamilto-

nians in order to describe the lowest magnetic (nonionic) states based on different sets of renormalized effective exchange and hopping parameters, which incorporate (some) correlation and spatial-symmetry effects.

#### IV. DISCUSSION

While it is our goal to determine these parameters either from our *ab initio* calculations (or even experimental data), it is instructive to compare them with the bare-integral, noncorrelated values of the mean-field Hamiltonian and the Coulomb repulsion over suitably chosen localized molecular orbitals (Table I). Notably, the values of these integrals for the Ni atom have also been discussed by Hubbard in his seminal paper [74], as well as by Victora and Falicov in their solution of the four-center tetragonal  $\text{Ni}_4$  cluster [72,75], and are consistent with our data in Table I. Let us turn first to the  $U = 0$  limit, which is easy to analyze analytically. Using values from Table I in Hamiltonians (7) and (8), we get a qualitative disagreement with our *ab initio* calculations on two marked features: (a) The predicted singlet-triplet splitting is much larger than the exchange splitting (for  $U = 0$  it is given by the  $t_a$  hopping constant; see discussion above), and (b) the exchange splitting itself is equal for the  $A_{2g}$ ,  $B_{2g}$ , and  $E_u$  blocks.

Our *third finding* is that turning on the on-site repulsion improves the energy scheme in several aspects. Figure 4(a)

TABLE I. The hopping, the Hubbard  $U$ , and the nearest-neighbor exchange integrals between the states of Eq. (4) *without* correlations [see also Fig. 4(b)]. The hopping between the  $d_{xz}$  states differs for the  $x$  and  $y$  directions (the same for  $d_{yz}$ ). Both numbers are given.

Orbitals	$t_{a,b}$ (eV)	$U_1$ (eV)	$J_1^{(0)}$ (meV)	$U_2$ (eV)	$J_2$ (meV)	$U_3$ (eV)	$J_3$ ( $\mu$ eV)
$d_{xy}$	0.93	26.80	566	7.48	16	5.21	599
$d_{z^2}$	0.91	22.49	896	6.64	29	4.64	997
$d_{xz}/d_{yz}$	0.95/−0.22	25.06	987	7.19	12	5.04	119
$d_{x^2-y^2}$	−2.33	26.37					
Atomic data <sup>a</sup>		16	1000				
Estimates <sup>b</sup>		20		6.	25		

<sup>a</sup>Taken from Refs. [72,73].

<sup>b</sup>Taken from Ref. [74].

depicts the energy eigenstates of the respective effective Hamiltonians for every irreducible representation for  $d_{xy} \rightarrow d_{x^2-y^2}$  excitations as functions of  $U$ . Interestingly, for symmetry reasons, for  $A_{1g}$  and  $B_{1g}$  the energies do not depend on  $U$ . Figure 4(c) shows the singlet-triplet splitting for two different sets of exchange parameters for the three irreducible representations for which we could clearly identify singlet-triplet pairs as functions of  $U$  [see Fig. 4(c)], namely,  $B_{2g}$  (purple),  $E_u$  (green), and  $A_{2g}$  (orange). The solid and dotted lines correspond to two different sets of exchange parameters.

An immediately obvious fact is that the splittings within every irreducible representation depend on  $U$ . The asymptotic values, however, are the same:  $\Delta E_0 \equiv \frac{1}{4}J_1 + \frac{1}{2}J_2 + \frac{1}{4}J_3$  in the noninteracting case and  $\Delta E_\infty \equiv J_1$  for  $U \rightarrow \infty$ . Despite this improvement, the ordering of states based on the original parameters [dotted lines in Fig. 4(c)] must be corrected. This is further achieved by switching on the nearest-neighbor and diagonal exchanges such that the condition  $\Delta E_0 > \Delta E_\infty$  is fulfilled (solid lines) and by setting the on-site repulsion to 10 eV. Ultimately, the best match to the *ab initio* calculations (the three colored triangles on the energy axis) is found for  $J_1 = 0.3$  eV,  $J_2 = 0.8$  eV,  $J_3 = 0.4$  eV, and  $U = 10$  eV (solid lines). These values differ significantly from the ones in Fig. 4(b), which are simply the values calculated as the integrals between the  $d$  orbitals since the latter ones do not include any electron screening, orbital relaxation, and correlation effects (compare also with Table I).

The physical properties of molecular magnets are set by the oxidation state of the constituent transition atoms and,

to a much lesser extent, by their mass. The oxidation state determines the filling of valence electronic shells (typically,  $s$  and  $d$ ). In turn, they contribute to the magnetic properties of the systems. The electronic configuration of Ni atoms is not uncommon for molecular magnets and can typically be associated with Cu II ions. Thus, isoelectronic counterparts of  $Ni_4$  can be found among synthesized molecular magnets [76].

## V. CONCLUSIONS

Summarizing, we propose a surprisingly efficient procedure to map a sophisticated first-principles treatment of electronic correlations to a few-parameter model Hamiltonian. For our paradigm system  $Ni_4$  we find three things: (a) We can subdivide the total Hilbert space in subspaces of irreducible representations and find several singlet-triplet pairs with approximately the same spatial wave function in each subspace. (b) In each subspace we can eliminate the nonmagnetic (ionic) states and derive a set of five effective parameters (three exchange and two hopping parameters) unique to each subspace. (c) Finally, in order to better match the first-principles level scheme we must switch on the on-site repulsion (Hubbard  $U$ ) as a sixth parameter. Our procedure already represents a tremendous advance in the theoretical treatment of finite, highly correlated molecular magnets.

Exploration of these effects offers exciting possibilities for further investigations in combination with well-established experimental techniques such as measurements and fitting of the magnetic susceptibility [77] or directly for individual clusters (rather than in an ensemble) with the micro-SQUID [69,70].

In a forthcoming publication we will discuss relativistic (fine-structure) effects (anisotropy of exchange vs breakdown of spin rotational invariance due to relativity).

## ACKNOWLEDGMENTS

This work is supported by the German Research Foundation (Deutsche Forschungsgemeinschaft, DFG) Collaborative Research Centre SFB/TRR 173 “Spin+X” (G.L. and Y.P.). W.H. acknowledges the hospitality of the nonequilibrium many-body systems group at Martin-Luther Universität Halle-Wittenberg during his sabbatical leave, where most of the first-principles calculations were performed.

- 
- [1] J. Simon, W. S. Bakr, R. Ma, M. E. Tai, P. M. Preiss, and M. Greiner, Quantum simulation of antiferromagnetic spin chains in an optical lattice, *Nature (London)* **472**, 307 (2011).
  - [2] A. O. Leonov and M. Mostovoy, Multiply periodic states and isolated skyrmions in an anisotropic frustrated magnet, *Nat. Commun.* **6**, 8275 (2015).
  - [3] A. Micheli, G. K. Brennen, and P. Zoller, A toolbox for lattice-spin models with polar molecules, *Nat. Phys.* **2**, 341 (2006).
  - [4] N. Nagaosa and Y. Tokura, Topological properties and dynamics of magnetic skyrmions, *Nat. Nanotechnol.* **8**, 899 (2013).
  - [5] I. Bloch, Ultracold quantum gases in optical lattices, *Nat. Phys.* **1**, 23 (2005).
  - [6] L. F. Livi, G. Cappellini, M. Diem, L. Franchi, C. Clivati, M. Frittelli, F. Levi, D. Calonico, J. Catani, M. Inguscio, and L. Fallani, Synthetic Dimensions and Spin-Orbit Coupling with an Optical Clock Transition, *Phys. Rev. Lett.* **117**, 220401 (2016).
  - [7] A. Furrer and O. Waldmann, Magnetic cluster excitations, *Rev. Mod. Phys.* **85**, 367 (2013).
  - [8] J. Schnack, M. Brüger, M. Luban, P. Kögerler, E. Morosan, R. Fuchs, R. Modler, H. Nojiri, R. C. Rai, J. Cao, J. L. Musfeldt, and

- X. Wei, Observation of field-dependent magnetic parameters in the magnetic molecule  $\text{Ni}_4\text{Mo}_{12}$ , *Phys. Rev. B* **73**, 094401 (2006).
- [9] K. Iida, S.-H. Lee, T. Onimaru, K. Matsubayashi, and T. J. Sato, Determination of spin Hamiltonian in the  $\text{Ni}_4$  magnetic molecule, *Phys. Rev. B* **86**, 064422 (2012).
- [10] E. Ruiz, A. Rodríguez-Forteza, J. Cano, S. Alvarez, and P. Alemany, About the calculation of exchange coupling constants in polynuclear transition metal complexes, *J. Comput. Chem.* **24**, 982 (2003).
- [11] E. Ruiz, A. Rodríguez-Forteza, J. Cano, and S. Alvarez, Theoretical study of exchange coupling constants in an  $\text{Fe}_{19}$  complex, *J. Phys. Chem. Solids* **65**, 799 (2004).
- [12] A. Furrer, A. Podlesnyak, and K. W. Krämer, Extraction of exchange parameters in transition-metal perovskites, *Phys. Rev. B* **92**, 104415 (2015).
- [13] E. Ruiz, A. Rodríguez-Forteza, J. Tercero, T. Cauchy, and C. Massobrio, Exchange coupling in transition-metal complexes via density-functional theory: Comparison and reliability of different basis set approaches, *J. Chem. Phys.* **123**, 074102 (2005).
- [14] E. Cremades, J. Cano, E. Ruiz, G. Rajaraman, C. J. Milios, and E. K. Brechin, Theoretical methods enlighten magnetic properties of a family of  $\text{Mn}_6$  single-molecule magnets, *Inorg. Chem.* **48**, 8012 (2009).
- [15] L. Noodleman, Valence bond description of antiferromagnetic coupling in transition metal dimers, *J. Chem. Phys.* **74**, 5737 (1981).
- [16] A. Bencini, F. Totti, C. A. Daul, K. Doclo, P. Fantucci, and V. Barone, Density functional calculations of magnetic exchange interactions in polynuclear transition metal complexes, *Inorg. Chem.* **36**, 5022 (1997).
- [17] D. Dai and M.-H. Whangbo, Spin exchange interactions of a spin dimer: Analysis of broken-symmetry spin states in terms of the eigenstates of Heisenberg and Ising spin Hamiltonians, *J. Chem. Phys.* **118**, 29 (2003).
- [18] A. Bencini and F. Totti, A few comments on the application of density functional theory to the calculation of the magnetic structure of oligo-nuclear transition metal clusters, *J. Chem. Theory Comput.* **5**, 144 (2009).
- [19] L. K. Thompson, O. Waldmann, and Z. Xu, Polynuclear manganese grids and clusters—A magnetic perspective, *Coord. Chem. Rev.* **249**, 2677 (2005).
- [20] M. L. Wall, K. Maeda, and L. D. Carr, Simulating quantum magnets with symmetric top molecules, *Ann. Phys. (Berlin, Ger.)* **525**, 845 (2013).
- [21] L. K. Thompson and L. N. Dawe, Magnetic properties of transition metal (Mn(II), Mn(III), Ni(II), Cu(II)) and lanthanide (Gd(III), Dy(III), Tb(III), Eu(III), Ho(III), Yb(III)) clusters and [n<sub>x</sub>n] grids: Isotropic exchange and SMM behaviour, *Coord. Chem. Rev.* **289–290**, 13 (2015).
- [22] R. A. Klemm and D. V. Efremov, Single-ion and exchange anisotropy effects and multiferroic behavior in high-symmetry tetramer single-molecule magnets, *Phys. Rev. B* **77**, 184410 (2008).
- [23] J. T. Haraldsen, T. Barnes, J. W. Sinclair, J. R. Thompson, R. L. Sacci, and J. F. C. Turner, Magnetic properties of a Heisenberg coupled-trimer molecular magnet: General results and application to spin-12 vanadium clusters, *Phys. Rev. B* **80**, 064406 (2009).
- [24] J. T. Haraldsen, Heisenberg Pentamer: Insights into Inelastic Neutron Scattering on Magnetic Clusters, *Phys. Rev. Lett.* **107**, 037205 (2011).
- [25] G. Houchins and J. T. Haraldsen, Generalization of polarized spin excitations for asymmetric dimeric systems, *Phys. Rev. B* **91**, 014422 (2015).
- [26] E. Livioiti, S. Carretta, and G. Amoretti, *S*-mixing contributions to the high-order anisotropy terms in the effective spin Hamiltonian for magnetic clusters, *J. Chem. Phys.* **117**, 3361 (2002).
- [27] S. Carretta, E. Livioiti, N. Magnani, P. Santini, and G. Amoretti, *S* Mixing and Quantum Tunneling of the Magnetization in Molecular Nanomagnets, *Phys. Rev. Lett.* **92**, 207205 (2004).
- [28] S. G. Tabrizi, A. V. Arbuznikov, and M. Kaupp, Construction of giant-spin hamiltonians from many-spin hamiltonians by third-order perturbation theory and application to an  $\text{Fe}_3\text{Cr}$  single-molecule magnet, *Chem. Eur. J.* **22**, 6853 (2016).
- [29] G. Lefkidis, G. P. Zhang, and W. Hübner, Angular Momentum Conservation for Coherently Manipulated Spin Polarization in Photoexcited NiO: An *Ab Initio* Calculation, *Phys. Rev. Lett.* **103**, 217401 (2009).
- [30] S. Heinze, K. von Bergmann, M. Menzel, J. Brede, A. Kubetzka, R. Wiesendanger, G. Bihlmayer, and S. Blügel, Spontaneous atomic-scale magnetic skyrmion lattice in two dimensions, *Nat. Phys.* **7**, 713 (2011).
- [31] J. R. Friedman, M. P. Sarachik, J. Tejada, and R. Ziolo, Macroscopic Measurement of Resonant Magnetization Tunneling in High-Spin Molecules, *Phys. Rev. Lett.* **76**, 3830 (1996).
- [32] W. Wernsdorfer, Quantum Phase Interference and Parity Effects in Magnetic Molecular Clusters, *Science* **284**, 133 (1999).
- [33] D. Gatteschi and R. Sessoli, Quantum tunneling of magnetization and related phenomena in molecular materials, *Angew. Chem., Int. Ed.* **42**, 268 (2003).
- [34] C. M. Ramsey, E. del Barco, S. Hill, S. J. Shah, C. C. Beedle, and D. N. Hendrickson, Quantum interference of tunnel trajectories between states of different spin length in a dimeric molecular nanomagnet, *Nat. Phys.* **4**, 277 (2008).
- [35] E. Burzurí, F. Luis, O. Montero, B. Barbara, R. Ballou, and S. Maegawa, Quantum Interference Oscillations of the Superparamagnetic Blocking in an  $\text{Fe}_8$  Molecular Nanomagnet, *Phys. Rev. Lett.* **111**, 057201 (2013).
- [36] Y. Chen, M. D. Ashkezari, C. A. Collett, R. A. Allão Cassaro, F. Troiani, P. M. Lahti, and J. R. Friedman, Observation of Tunneling-Assisted Highly Forbidden Single-Photon Transitions in a  $\text{Ni}_4$  Single-Molecule Magnet, *Phys. Rev. Lett.* **117**, 187202 (2016).
- [37] L. Bogani and W. Wernsdorfer, Molecular spintronics using single-molecule magnets, *Nat. Mater.* **7**, 179 (2008).
- [38] J. R. Friedman and M. P. Sarachik, Single-molecule nanomagnets, *Annu. Rev. Condens. Matter Phys.* **1**, 109 (2010).
- [39] P. Bruno, Berry Phase, Topology, and Degeneracies in Quantum Nanomagnets, *Phys. Rev. Lett.* **96**, 117208 (2006).
- [40] S. J. Blundell, Molecular magnets, *Contemp. Phys.* **48**, 275 (2007).
- [41] S. Carretta, T. Guidi, P. Santini, G. Amoretti, O. Pieper, B. Lake, J. van Slageren, F. El Hallak, W. Wernsdorfer, H. Mutka, M. Russina, C. J. Milios, and E. K. Brechin, Breakdown of the Giant Spin Model in the Magnetic Relaxation of the  $\text{Mn}_6$  Nanomagnets, *Phys. Rev. Lett.* **100**, 157203 (2008).
- [42] R. Maurice, C. de Graaf, and N. Guihéry, Theoretical determination of spin Hamiltonians with isotropic and

- anisotropic magnetic interactions in transition metal and lanthanide complexes, *Phys. Chem. Chem. Phys.* **15**, 18784 (2013).
- [43] C. Rudowicz and M. Karbowiak, Disentangling intricate web of interrelated notions at the interface between the physical (crystal field) Hamiltonians and the effective (spin) Hamiltonians, *Coord. Chem. Rev.* **287**, 28 (2015).
- [44] T. Gupta and G. Rajaraman, Modelling spin Hamiltonian parameters of molecular nanomagnets, *Chem. Commun.* **52**, 8972 (2016).
- [45] W. Hübner, S. Kersten, and G. Lefkidis, Optical spin manipulation for minimal magnetic logic operations in metallic three-center magnetic clusters, *Phys. Rev. B* **79**, 184431 (2009).
- [46] H. Xiang, G. Lefkidis, and W. Hübner, Unified theory of ultrafast femtosecond and conventional picosecond magnetic dynamics in the distorted three-center magnetic cluster  $\text{Ni}_3\text{Na}_2$ , *Phys. Rev. B* **86**, 134402 (2012).
- [47] W. Jin, C. Li, G. Lefkidis, and W. Hübner, Laser control of ultrafast spin dynamics on homodinuclear iron- and nickel-oxide clusters, *Phys. Rev. B* **89**, 024419 (2014).
- [48] D. Chaudhuri, H. P. Xiang, G. Lefkidis, and W. Hübner, Laser-induced ultrafast spin dynamics in di-, tri- and tetranuclear nickel clusters, and the M process, *Phys. Rev. B* **90**, 245113 (2014).
- [49] C. Li, J. Liu, S. Zhang, G. Lefkidis, and W. Hübner, Strain assisted ultrafast spin switching on  $\text{Co}_2@C_{60}$  endohedral fullerenes, *Carbon* **87**, 153 (2015).
- [50] W. Metzner and D. Vollhardt, Correlated Lattice Fermions in  $d = \infty$  Dimensions, *Phys. Rev. Lett.* **62**, 324 (1989).
- [51] D. Vollhardt, Dynamical mean-field theory for correlated electrons, *Ann. Phys. (Berlin, Ger.)* **524**, 1 (2012).
- [52] A. Georges, G. Kotliar, W. Krauth, and M. J. Rozenberg, Dynamical mean-field theory of strongly correlated fermion systems and the limit of infinite dimensions, *Rev. Mod. Phys.* **68**, 13 (1996).
- [53] X. López, M.-Y. Huang, G.-C. Huang, S.-M. Peng, F.-Y. Li, M. Bénard, and M.-M. Rohmer, Even-numbered metal chain complexes: Synthesis, characterization, and DFT analysis of  $[\text{Ni}_4(\mu_4\text{-Tsdpda})_4(\text{H}_2\text{O})_2]$  ( $\text{Tsdpda}^{2-} = n\text{-}(p\text{-toluenesulfonyl})\text{dipyridyldiamido}$ ),  $[\text{Ni}_4(\mu_4\text{-Tsdpda})_4]^+$ , and related  $\text{Ni}_4$  string complexes, *Inorg. Chem.* **45**, 9075 (2006).
- [54] M. Fondo, N. Ocampo, A. M. García-Deibe, R. Vicente, M. Corbella, M. R. Bermejo, and J. Sanmartín, Self-assembly of a tetranuclear  $\text{Ni}_4$  cluster with an  $s = 4$  ground state: The first  $3d$  metal cluster bearing a  $\mu_4 - \eta^2:\eta^2\text{-O}_2\text{O}$  carbonate ligand, *Inorg. Chem.* **45**, 255 (2006).
- [55] N. Kirchner, J. van Slageren, B. Tsukerblat, O. Waldmann, and M. Dressel, Antisymmetric exchange interactions in  $\text{Ni}_4$  clusters, *Phys. Rev. B* **78**, 094426 (2008).
- [56] D. Chaudhuri, G. Lefkidis, and W. Hübner, All-spin-based ultrafast nanologic elements with a  $\text{Ni}_4$  cluster, *Phys. Rev. B* **96**, 184413 (2017).
- [57] W. Jin, M. Becherer, D. Bellaire, G. Lefkidis, M. Gerhards, and W. Hübner, Infrared and electronic absorption spectra as well as ultrafast spin dynamics in isolated  $\text{Co}_3^+(\text{EtOH})$  and  $\text{Co}_3^+(\text{EtOH}, \text{H}_2\text{O})$  clusters, *Phys. Rev. B* **89**, 144409 (2014).
- [58] D. Chaudhuri, W. Jin, G. Lefkidis, and W. Hübner, Ab initio theory for femtosecond spin dynamics, angle-resolved fidelity analysis, and the magneto-optical Kerr effect in the  $\text{Ni}_3(\text{CH}_3\text{OH})$  and  $\text{Co}_3^+(\text{CH}_3\text{OH})$  clusters, *J. Chem. Phys.* **143**, 174303 (2015).
- [59] K. H. Meiwes-Broer, *Metal Clusters at Surfaces* (Springer, Berlin, 2000).
- [60] P. W. Anderson, Antiferromagnetism. Theory of superexchange interaction, *Phys. Rev.* **79**, 350 (1950).
- [61] J. B. Goodenough, An interpretation of the magnetic properties of the perovskite-type mixed crystals  $\text{La}_{1-x}\text{Sr}_x\text{CoO}_{3-\lambda}$ , *J. Phys. Chem. Solids* **6**, 287 (1958).
- [62] J. Kanamori, Theory of the magnetic properties of ferrous and cobaltous oxides, I, *Prog. Theor. Phys.* **17**, 177 (1957).
- [63] J. Kanamori, Theory of the magnetic properties of ferrous and cobaltous oxides, II, *Prog. Theor. Phys.* **17**, 197 (1957).
- [64] T. Noro, M. Sekiya, and T. Koga, Segmented contracted basis sets for atoms H through Xe: Sapporo-(DK)- $n$  ZP sets ( $n = \text{D, T, Q}$ ), *Theor. Chem. Acc.* **131**, 1124 (2012).
- [65] M. W. Schmidt, K. K. Baldrige, J. A. Boatz, S. T. Elbert, M. S. Gordon, J. H. Jensen, S. Koseki, N. Matsunaga, K. A. Nguyen, S. Su, T. L. Windus, M. Dupuis, and J. A. Montgomery, General atomic and molecular electronic structure system, *J. Comput. Chem.* **14**, 1347 (1993).
- [66] F. Neese, The ORCA program system, *Wiley Interdiscip. Rev. Comput. Mol. Sci.* **2**, 73 (2012).
- [67] Lowering the symmetry induces additional magnetic anisotropy and reduces the number of irreducible representations. Results for  $\text{Ni}_4$  in lower symmetry will be presented in a future publication.
- [68] A. I. Krylov, Equation-of-motion coupled-cluster methods for open-shell and electronically excited species: The hitchhiker's guide to Fock space, *Rev. Phys. Chem.* **59**, 433 (2008).
- [69] M. Jamet, W. Wernsdorfer, C. Thirion, D. Mailly, V. Dupuis, P. Mélinon, and A. Pérez, Magnetic Anisotropy of a Single Cobalt Nanocluster, *Phys. Rev. Lett.* **86**, 4676 (2001).
- [70] W. Wernsdorfer, From micro- to nano-SQUIDS: Applications to nanomagnetism, *Supercond. Sci. Technol.* **22**, 064013 (2009).
- [71] Y. Pavlyukh, M. Schüler, and J. Berakdar, Single- or double-electron emission within the Keldysh nonequilibrium Green's function and Feshbach projection operator techniques, *Phys. Rev. B* **91**, 155116 (2015).
- [72] R. H. Victora and L. M. Falicov, Exact Solution of a Four-Site  $d$ -Electron Problem: The Nickel-Metal Photoemission Spectrum, *Phys. Rev. Lett.* **55**, 1140 (1985).
- [73] C. E. Moore, *Atomic Energy Levels* (U.S. National Bureau of Standards, Washington, D.C., 1971), Vol. 2, p. 98.
- [74] J. Hubbard, Electron correlations in narrow energy bands, *Proc. R. Soc. London, Ser. A* **276**, 238 (1963).
- [75] L. M. Falicov and R. H. Victora, Exact solution of the Hubbard model for a four-center tetrahedral cluster, *Phys. Rev. B* **30**, 1695 (1984).
- [76] P. Happ, C. Plenk, and E. Rentschler, 12-MC-4 metallocrowns as versatile tools for SMM research, *Coord. Chem. Rev.* **289–290**, 238 (2015).
- [77] O. Kahn, *Molecular Magnetism* (VCH, New York, 1993).